International Journal of Heat and Fluid Flow 30 (2009) 237–248

Contents lists available at ScienceDirect

International Journal of Heat and Fluid Flow

journal homepage: www.elsevier.com/locate/ijhff

Conjugate turbulent heat transfer in a square cavity with a solar control coating deposited to a vertical semitransparent wall

J. Xamán [a,*], G. Álvarez [a], J. Hinojosa [b,1], J. Flores [a]

[a] Centro Nacional de Investigación y Desarrollo Tecnológico, CENIDET-DGEST-SEP, Prol. Av. Palmira S/N. Col. Palmira, Cuernavaca, Morelos CP 62490, Mexico
[b] Universidad de Sonora – UNISON, Blvd. Luis Encinas y Rosales, Col. Centro, Hermosillo, Sonora CP 83000, Mexico

ARTICLE INFO

Article history:
Received 15 March 2008
Received in revised form 17 October 2008
Accepted 17 November 2008
Available online 12 January 2009

Keywords:
Natural convection
Radiative exchange
κ-ε turbulent model

ABSTRACT

This paper presents a numerical study of the conjugate heat transfer (natural convection, surface thermal radiation and conduction) in a square cavity with turbulent flow. The cavity has one vertical isothermal wall, two horizontal adiabatic walls and one vertical semitransparent wall with a selective coating applied to the inner side to control the solar radiation transmission. Later on the semitransparent wall is replaced with another one without the selective coating. The mathematical model for the turbulent flow in the cavity was solved using the finite volume method. The system had the following conditions: the uniform temperature in the isothermal wall was 21 °C, the external ambient temperature was fixed at 35 °C and on the semitransparent wall the direct normal solar irradiation of 750 W/m^2 was considered constant. The Rayleigh number was varied in the range of $10^9 \leqslant Ra \leqslant 10^{12}$ by changing the lengths of the cavity from 0.70 m to 6.98 m, respectively. The results show that, even though the air temperature of the cavity with the solar control film coating semitransparent wall (case A) is higher compared with the one without solar film coating (case B), the total amount of heat going through the cavity is lower compared to the one going through the cavity without solar control film. The total amount of energy transferred to the air in cavity for the case A was 41.98% less than for the case B. A set of correlations for the Nusselt number was obtained for both cases considering the conjugate heat transfer.

1. Introduction

Natural convection inside a square closed cavity with two vertical isothermal walls and two horizontal adiabatic walls is a classical problem for natural convection, and it has applications in several technological fields, like cooling of electronic equipment, flat solar collectors, thermal design of buildings, etc.

In the study of thermal design of buildings, and its components, such as walls, floor, ceiling, windows and rooms as cavities can be analyzed by theoretical and experimental methods. The advantage is the reduction of the real system into an abstract model that allows the manipulation of the components and the physical properties of the construction materials. Theoretical methods can be classified depending on how the governing equations are obtained, overall, differential and integral models. In most cases, the analytical solution is complex and sometimes impossible to obtain, thus, numerical methods have to be used to calculate parameters like the overall heat transfer coefficients which are required in commercial software based on overall theoretical models for building thermal design.

Several papers have reported numerical studies for laminar flows in closed cavities, considering the combined three mechanisms of heat transfer (natural convection, thermal radiation and conduction). Larson and Viskanta (1976) studied numerically the conjugate heat transfer in a square closed cavity with opaque and diffuse walls. The results of Larson and Viskanta shows that the thermal radiation is the dominant heat transfer mechanism and it modifies the flow pattern significantly. In the study of Webb and Viskanta (1987), they included a vertical semitransparent wall (glass sheet) in the cavity. Their results revealed that the 70% of the incoming energy to the system was provided by the direct absorption of thermal radiation. Behnia et al. (1990) also considered a rectangular cavity with semitransparent wall. The semitransparent wall had convective losses to the surroundings. The results of Behnia et al. indicated, that the external convection debilitates the internal flow circulation, the thermal radiation grows up and the combination of this heat transfer modes produces an increasing effect for the internal circulation. Kwon et al. (1993) presented the effect of considering a semitransparent window in the middle of vertical wall in the closed cavity. Their results show that the temperature profiles in the adiabatic wall increases its values with the increment of the transmittance of the semitransparent window.

* Corresponding author. Tel./fax: +52 777 3 62 77 70.
E-mail addresses: jxaman@cenidet.edu.mx (J. Xamán), xaman9745@hotmail.com (J. Xamán), gaby@cenidet.edu.mx (G. Álvarez), fhinojosa@iq.uson.mx (J. Hinojosa), jasson@cenidet.edu.mx (J. Flores).
[1] Tel.: +52 662 2 59 21 05.

0142-727X/$ - see front matter © 2008 Elsevier Inc. All rights reserved.
doi:10.1016/j.ijheatfluidflow.2008.11.004

Nomenclature

$dF_{dA_i-dA_j}$	view factor between elements *i–j*
C_p	specific heat (J/kg K)
$C_{1\varepsilon}$, $C_{2\varepsilon}$, $C_{3\varepsilon}$, C_μ	coefficients of the turbulence model
g^*	gravitational acceleration (9.81 m/s^2)
G	solar radiation (W/m^2)
G_k	buoyancy production/destruction of kinetic energy
h_{ext}	convective heat transfer coefficient at the outside glass wall (W/m^2 K)
H	height of the cavity (m)
L	length of the cavity (m)
L_g	thickness of the glass (m)
Nu	Nusselt number
P	pressure (Pa)
P_K	turbulence kinetic energy production
Pr	Prandtl Number (ν/α)
q	heat flux (W/m^2)
Ra	Rayleigh number, ($g^*\beta\Delta TL^3/\nu\alpha$)
s_g	extinction coefficient (m^{-1})
T	temperature (K)
T_2	cold wall temperature (K)
T_4	inside average temperature of the glass wall (K)
T_0	reference temperature [$(T_4 + T_2)/2$] (K)
u, v	dimensional horizontal and vertical velocities (m/s)
x, y	dimensional coordinates, m
x^*, y^*	dimensionless coordinates, x/H, y/H
z	stretching factor of grid

Greek symbols

α	thermal diffusivity (m^2/s)
α^*	absorptivity
β	thermal expansion coefficient (K^{-1})
ΔT	temperature difference ($T_4 - T_2$) (K)
ε	rate of dissipation of κ (m^2/s^3)
ε^*	emissivity
κ	turbulence kinetic energy (m^2/s^2)
λ	thermal conductivity (W/m K)
μ	dynamic viscosity (kg/m/s)
μ_t	turbulent viscosity (kg/m/s)
ν	kinematic viscosity (m^2/s)
ρ	density (kg/m^3)
ρ^*	reflectivity
σ	Stefan–Boltzman constant, 5.670×10^{-8} W/m^2 K^4
σ_T	turbulent Prandtl number
σ_k	Prandtl number for k
σ_ε	Prandtl number for ε
τ^*	transmissivity

Subscripts

a	air
ext	ambient
cond	conductive
conv	convective
f	film
g	glass wall
int	inside
o	outside
rad	radiative
Sys	system
total	total quantities

Álvarez and Estrada (2000) considered, besides the semitransparent wall a solar control film adhered to the inside surface of the semitransparent wall. The comparison of the laminar air flow patterns between the effect of using clear glass and coated film glass in the cavity showed that they are similar qualitatively but different quantitatively. The authors show that the total energy transferred to the air in the cavity through the glass with solar control coating is lower than the one through the plain clear glass.

On the other hand, there are very few studies dealing with conjugate turbulent natural convection and surface thermal radiation in cavities with semitransparent walls. The problem of turbulent flow in a closed cavity with surface thermal radiation was studied by Velusamy et al. (2001) considering a differentially heated cavity with opaque and diffuse walls. Their results indicated that the interaction between the radiative surfaces increases the magnitude of velocities and the turbulence levels in the vertical and horizontal boundary layers, increasing the convective heat transfer about 25%. Ampofo and Karayiannis (2003) reported an experimental study of low-level turbulence natural convection in an air filled vertical square cavity. The local velocity and temperature were presented at different locations in the cavity. The authors mentioned that the quantities are almost negligible in the conductive layer, which confirms that the heat transfer in this region of the boundary layer happens by pure conduction. The study also shows that the κ-ε model and LES can predict the mean quantities such as velocity and temperature in the cavity reasonably well and that LES predicts the flow quantities much better that the κ-ε model. They concluded that the results can be useful as benchmark data for comparison with CFD codes. Xamán and Álvarez (2006) determined the influence of the semitransparent glazing with and without SnS–Cu$_x$S solar control coating on turbulent natural convection in a square cavity. The results show that direct solar energy transmittance of the semitransparent glazing with film coating is much lower than the one without solar control coating, thus the total heat gain through the glazing with solar control coating would be lower than the one without solar control coating. Anil Kumar Sharma et al. (2007) investigated the conjugate turbulent natural convection and surface radiation in rectangular enclosures heated from below and cooled from other walls. The Rayleigh number based on the width of the enclosure was varied from 10^8 to 10^{12} and the aspect ratio was varied from 0.5 to 2.0. Detailed results including streamlines, temperature profiles, and overall Nusselt number were presented. The authors concluded that the surface thermal radiation is found to dampen natural convection and as a result the convective contribution to the heat transfer is reduced by ≈18–27%. However, this reduction in the convection effect is mainly compensated by the contribution of radiation; these results emphasize the need for coupling radiation and convection for accurate prediction of heat transfer in enclosures. Recently, Xamán et al. (2008) studied the conjugate heat transfer (laminar and turbulent natural convection, surface thermal radiation and conduction) in a square cavity with a glass wall. The Rayleigh number was varied in the range of $10^3 \leqslant Ra \leqslant 10^{12}$. Results showed that the flow pattern is not symmetric due to the combined effect of non-isothermal glass wall and radiative exchange inside the cavity and if the surface thermal radiation is neglected, significant under estimations in the total heat transfer is found. A correlation for the total Nusselt number was presented for both laminar and turbulent flow considering conjugate heat transfer.

As it is shown in the literature review, detailed studies of fluid flow and conjugate heat transfer inside an enclosure with a semitransparent wall are scarce due to its complexity; therefore more comprehensive studies are required. In this work we consider a detailed study of fluid flow and heat transfer by turbulent natural

convection and surface thermal radiation in a square cavity with a semitransparent wall with and without a solar control film. The objectives of this study are: to advance in the knowledge to obtain the thermal parameters approaching the real size rooms and to evaluate the thermal effect of using the semitransparent wall with and without a solar control film on the airflow in the cavity. A Rayleigh number range from 10^9 to 10^{12} was chosen for the heat transfer study in a square cavity. The Rayleigh number is based on the difference between the temperatures of the vertical walls, using the inside average temperature of the semitransparent wall (T_4). Turbulent natural convection and surface thermal radiation equations were solved simultaneously using the finite volume method and the net radiation method. The mathematical model considered includes the surface thermal radiation among the four walls and the heat transfer conduction through the semitransparent wall. Flow and temperature patterns are discussed and values of the Nusselt number as a function of the Rayleigh number are presented.

2. Physical model and assumptions

The heat transfer and the fluid flow in a two-dimensional closed square cavity of length L, was considered as it is shown in the schematic diagram of Fig. 1. If the cavity is thought as a long cavity in its third dimension normal to the paper, the two-dimensional assumption can be valid. The thermal fluid was assumed to be air in turbulent regime, initially at rest and with a uniform temperature. The cavity is formed by two horizontal adiabatic walls, one vertical isothermal wall and one semitransparent wall consisting of glass and a solar control film adhered to the inside surface. On the semitransparent wall an incoming normal uniform and constant solar radiation flux (750 W/m^2) is considered and two-dimensional heat transfer by conduction is taken into account. The assumption of top and bottom horizontal adiabatic walls is an approach; we assumed that the average temperatures of the top and lower rooms are nearly the same as the middle room, so the heat flux can be considered zero. The isothermal wall is not considered adiabatic; there may exit a thermal potential, because the left room may have a controlled temperature.

The properties of the air were assumed constant except for the density in the buoyancy force term in the momentum equations, according to the Boussinesq approximation. The thermal fluid was considered radiatively non-participating (dry air) and the opaque and the semitransparent walls of the cavity were considered as gray diffuse surfaces. It is well known that a glass reflects in a specular manner, but inside an enclosure there are multiple reflections and the directionality of each reflection is lost considering the heat fluxes in the boundaries. The optical properties considered are the integrated solar spectrum values. It is known that the glass transmittance and reflectance as a function of the solar incident angle is almost constant for angles less than 60°. The film solar control coating selected is SnS–Cu$_x$S.

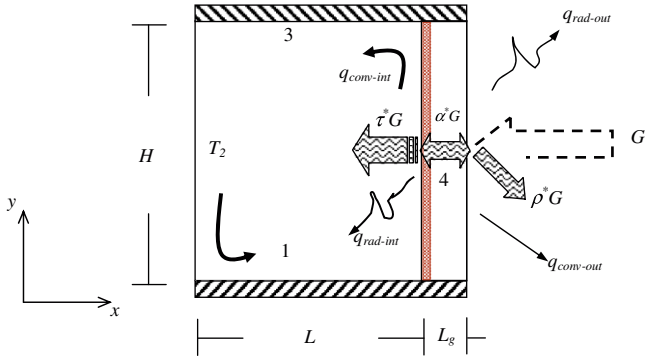

Fig. 1. Physical model of the square cavity with semitransparent wall.

3. Governing equations and boundary conditions

3.1. Turbulent natural-convection model

The steady state conservation equations governing the transport of mass, momentum and energy in primitive variables of an incompressible fluid, are expressed as

$$\frac{\partial(\rho u_i)}{\partial x_i} = 0 \tag{1}$$

$$\frac{\partial(\rho u_j u_i)}{\partial x_j} = -\frac{\partial P}{\partial x_i} + \frac{\partial}{\partial x_j}\left(\mu\frac{\partial u_i}{\partial x_j} - \rho\overline{u_i' u_j'}\right) - \rho\beta(T - T_0)g_i^* \tag{2}$$

$$\frac{\partial(\rho u_i T)}{\partial x_i} = \frac{\partial}{\partial x_i}\left(\frac{\lambda}{C_p}\frac{\partial T}{\partial x_i} - \rho\overline{u_i' T'}\right) \tag{3}$$

The above equations system is not complete because of the presence of the unknown Reynolds stress tensor ($\rho\overline{u_i' u_j'}$) in the momentum equation and the turbulent heat vector ($\rho u_i' T'$) in the energy equation. In the eddy viscosity model (EVM) the Reynolds stress tensor is modeled through the Boussinesq hypothesis as

$$\rho\overline{u_i' u_j'} = -\mu_t\left(\frac{\partial u_i}{\partial x_j} + \frac{\partial u_j}{\partial x_i}\right) + \frac{2}{3}\rho k\delta_{ij} \tag{4}$$

The high Reynolds number model (HRN) establishes that the turbulent viscosity (μ_t) can be obtained as

$$\mu_t = C_\mu\frac{\rho k^2}{\varepsilon} \tag{5}$$

where C_μ is a constant. The turbulent heat vector is modeled as follow:

$$\rho\overline{u_i' T'} = -\frac{\mu_t}{\sigma_T}\frac{\partial T}{\partial x_i} \tag{6}$$

where σ_T is the turbulent Prandtl number and δ_{ij} is the Kronecker delta. The turbulent viscosity can be related with the turbulent kinetic energy (κ) and the turbulent dissipation of kinetic energy (ε) through the empiric equation of Kolmorogov–Prandtl (Pope, 2000). The turbulent kinetic energy and the turbulent dissipation of kinetic energy can be obtained using its corresponding transport equation:

$$\frac{\partial(\rho u_i k)}{\partial x_i} = \frac{\partial}{\partial x_i}\left[\left(\mu + \frac{\mu_t}{\sigma_k}\right)\frac{\partial k}{\partial x_i}\right] + P_k + G_k - \rho\varepsilon \tag{7}$$

$$\frac{\partial(\rho u_i \varepsilon)}{\partial x_i} = \frac{\partial}{\partial x_i}\left[\left(\mu + \frac{\mu_t}{\sigma_\varepsilon}\right)\frac{\partial \varepsilon}{\partial x_i}\right] + [C_{1\varepsilon}(P_k + C_{3\varepsilon}G_\kappa) - C_{2\varepsilon}\rho\varepsilon]\frac{\varepsilon}{k} \tag{8}$$

where P_k and G_k are the production of turbulent kinetic energy by shearing and the generation/destruction by buoyancy.

The mathematical boundary conditions for the fluid domain are as follow:

Momentum boundary conditions:

$$\begin{aligned} u(0,y) &= u(L,y) = 0 \\ u(x,0) &= u(x,H) = 0 \\ v(0,y) &= v(L,y) = 0 \\ v(x,0) &= v(x,H) = 0 \end{aligned} \tag{9}$$

Energy boundary conditions:

$$\text{Bottom wall}: q_{conv\text{-}1} + q_{rad\text{-}1} = 0 \tag{10}$$

$$\text{Isothermal vertical wall}: T(0,y) = T_2 \tag{11}$$

$$\text{Upper wall}: q_{conv\text{-}3} + q_{rad\text{-}3} = 0 \tag{12}$$

$$\text{Semitransparent vertical wall}: q_{abs} + q_{cond\text{-}g\text{-}4} = q_{conv\text{-}4} + q_{rad\text{-}4} \tag{13}$$

where $q_{conv\text{-}1}$, $q_{conv\text{-}3}$ and $q_{conv\text{-}4}$ are the convection heat transfer fluxes from the inside surface to the adjacent fluid on walls 1, 3 and 4, respectively. The terms $q_{rad\text{-}1}$, $q_{rad\text{-}3}$ and $q_{rad\text{-}4}$ are the net radiative heat transfer fluxes at walls 1, 3 and 4. The term q_{abs} is the thermal energy that is absorbed by the solar control film of the glazing. Finally, $q_{cond\text{-}g\text{-}4}$ is the heat flux by heat conduction through the semitransparent wall.

The boundary conditions and coefficient values for k-ε turbulence model are: $k_w = 0.0$, $\varepsilon_w = \infty$, $C_\mu = 0.09$, $C_{1\varepsilon} = 1.44$, $C_{2\varepsilon} = 1.92$, $\sigma_k = 1.0$, $\sigma_\varepsilon = 1.3$ and $C_{3\varepsilon} = \tanh|v/u|$ (Henkes et al., 1991).

3.2. Conduction model of the semitransparent wall

In order to obtain the temperature profile inside the semitransparent wall formed by glass ($L_g = 6$ mm) with a thin solar control film coating, a differential energy balance was carried out. The model solution is used to determine the conductive heat flux of wall 4 ($q_{cond\text{-}g\text{-}4}$).

The heat transfer conduction equation for the differential element of the semitransparent wall is given by:

$$\frac{\partial}{\partial x_i}\left(\frac{\lambda_g}{C_{pg}}\frac{\partial T_g}{\partial x_i}\right) + \frac{1}{C_{pg}}\frac{d\Theta}{dx} = 0 \tag{14}$$

where Θ is the attenuation energy function by absorption and scattering, which depends on the extinction coefficient (s_g) as follows (Modest, 1993):

$$\Theta(x) = G\exp[-s_g(L_g - x)] \tag{15}$$

The outside boundary condition for the semitransparent wall at ($x = L + L_g$) can be expressed as

$$-\lambda_g\frac{\partial T_g}{\partial x} = h_{ext}[T_g - T_{ext}] + \sigma\varepsilon_g^*[T_g^4 - T_{ext}^4] \tag{16}$$

where T_{ext} is the external surroundings temperature. The film thickness (≈6 μm) was considered negligible with regard to the glass thickness (6 mm). In order to obtain the film temperature (T_f) at ($x = L$), the following energy balance at the film was carried out:

$$\alpha_f^*\tau_g^* G = -\lambda_g\frac{\partial T_g}{\partial x} + \lambda_a\frac{\partial T}{\partial x} + q_{rad\text{-}4} \tag{17}$$

where $T_f = T_g(0,y)$.

3.3. Radiation model

The net radiative method was used to calculate the resulting heat fluxes from the radiative exchange (Modest, 1993). The thermal radiative exchange between the cavity surfaces is shown in Fig. 2, using two differential areas on surfaces 1 and 2. The cavity surfaces are assumed opaque and diffuse except for the vertical right wall which is a semitransparent wall.

The radiative heat transfer from a surface is defined as the difference between the outgoing thermal radiation (radiosity) and the incoming thermal radiation (irradiance). Therefore making an energy balance over the differential element dA_k, located in r_k position on wall 1 (Fig. 2), we can obtain the resulting heat radiative flux for wall 1:

$$q_{rad\text{-}1}(x_1) = q_{o_1}(x_1) - q_{i_1}(x_1) \tag{18}$$

Because radiosity is defined for a diffuse opaque surface as the sum of emitted energy and reflected energy, which can be formulated as

$$q_{o_1}(x_1) = \varepsilon_1^*\sigma T_1^4(x_1) + \rho_1^* q_{i_1}(x_1) \tag{19}$$

The irradiance is defined as the sum of energy fractions outgoing from cavity surfaces differential elements that arrives to the analyzed surface. The irradiance mathematical formulation for a surface element i on wall 1 is given by:

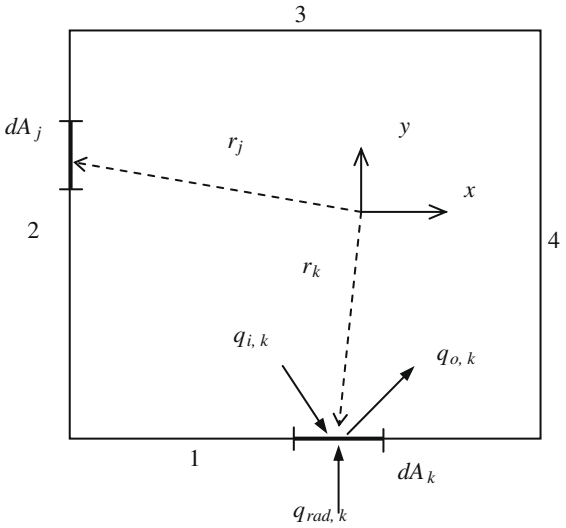

Fig. 2. Radiative balances in differential areas.

$$q_{i_1}(x_1) = \sum_{j=1}^{m}\int_{A_j} q_{o_j}(x_j)\,dF_{dA_1-dA_j} \tag{20}$$

where the summation over the jth surface element is to be taken for those elements over the boundary for which i interacts radiatively, $q_{i_1}(x_1)$ is the incoming thermal radiation over the differential element i on wall 1, x_1 is the element position on wall 1, $q_{o_j}(x_j)$ is the radiosity of cavity surfaces differential elements and $dF_{dA_1-dA_j}$ is the corresponding differential view factor. The view factors equations for the same configuration are reported by Álvarez and Estrada (2000). Therefore, substituting Eq. (20) into Eq. (19) together with the corresponding view factor equation, gives the radiosity equation for wall 1:

$$q_{o_1}(x_1) = \varepsilon_1^*\sigma T_1^4(x_1) + \frac{\rho_1^*}{2}\left\{\int_0^H \frac{q_{o_2}(y_2)x_1 y_2}{(x_1^2+y_2^2)^{3/2}}dy_2 + \int_0^L \frac{q_{o_3}(x_3)H^2}{(H^2+(x_3-x_1)^2)^{3/2}}dx_3 + \int_0^H \frac{q_{o_4}(y_4)(L-x_1)y_4}{(y_4^2+(L-x_1)^2)^{3/2}}dy_4\right\} \tag{21}$$

Similar equations can be derived for the remaining opaque cavity walls.

3.4. Thermal parameters

The Nusselt number is defined as the ratio between the convective or radiative heat transfer and the pure conduction heat transfer (Oosthuizen and Naylor, 1999), then:

$$Nu = \frac{q}{q_{cond}} \quad \text{if} \quad q = \begin{cases} q_{conv} & \Rightarrow \quad Nu_{conv} \\ q_{rad} & \Rightarrow \quad Nu_{rad} \end{cases} \tag{22}$$

where the conductive heat transfer through the system is given by $q_{cond} = \lambda_a(T_4 - T_2)/L$, the convective heat transfer from surface 4 to the internal fluid can be calculated as $q_{conv} = h(T_4 - T_2) = \lambda_a\frac{\partial T}{\partial x}\big|_4$ and q_{rad} is the net radiative heat transfer from surface 4.

A total Nusselt number was defined to consider the total heat transfer (including convection and radiation) as

$$Nu_{total} = Nu_{conv} + Nu_{rad} \tag{23}$$

A standard parameter used to describe the thermal behavior of windows formed with glass sheets and exposed to solar radiation is the solar heat gain coefficient (SHGC). The SHGC coefficient is defined as the ratio of the sum of transmitted direct solar energy and transmit-

ted heat transfer trough the window and the incident solar energy, in mathematical form (ASHRAE Handbook Fundamentals, 2005):

$$\mathrm{SHGC} = \frac{[q_{int} + \tau^* G]_{(glass+film)}}{G} \tag{24}$$

where, $\tau^* G$ is the direct solar energy transmitted through the glazing, G is the incident solar energy at the outside of the glazing and q_{int} is the convective and radiative heat flux toward the interior from the glazing, which is expressed as

$$q_{int} = q_{conv} + q_{rad} \tag{25}$$

4. Numerical algorithm

4.1. Discretization

The governing equations of the convective and conductive model described above are numerically solved using the finite volume method (Patankar, 1980). In order to implement the numerical algorithm, the governing equations can be represented by the following general equation of convection–diffusion:

$$\frac{\partial}{\partial x_j}(\rho u_j \phi) = \frac{\partial}{\partial x_j}\left(\Gamma \frac{\partial \phi}{\partial x_j}\right) + S_\phi \tag{26}$$

The integration of Eq. (26) over the corresponding finite volume and substitution of every term by discrete values of ϕ in the nodal points gives the following algebraic equation for every nodal point:

$$a_P \phi_P^{n+1} = \sum_{nb=E,O,N,S} a_{nb} \phi_{nb}^{n+1} + b^n \tag{27}$$

where n is the iteration number, nb are the neighbor coefficients, b is the source term and ϕ represents the discrete value of dependent variable of the control volume.

The position of the nodes of a grid is calculated using a stretching function so that the nodes are closer to each other near the walls of the cavity. The velocity components are calculated at a staggered grid while the scalar variables are calculated at the main grid (not staggered). The convective terms are discretized applying the hybrid scheme and the diffusive terms with the central difference scheme (low order scheme). The coupling between the momentum and continuity equations is made with the SIMPLEC algorithm (Van Doormaal and Raithby, 1984). The algebraic equations system obtained with Eq. (27) is solved applying the line by line method (LBL) with alternating direction implicit scheme (ADI). Furthermore under-relaxation is introduced using the false transient strategy (Mallison and de Vahl Davis, 1973). If the values in the mass balance for every control volume as well as the residual values of the different equations are sufficiently low, overall convergence is obtained (typically 10^{-10}). The above convergence criterion assures an acceptable solution. A radiative balance at the walls is solved using an iterative approach in order to couple turbulent natural convection to surface thermal radiation effect at the boundaries. The view factors between the elements were determined by using the equations reported by Álvarez and Estrada (2000). The radiosity equations were solved by Simpson's rule.

The general procedure for the conjugate heat transfer in a cavity can be summarized in the following steps: (1) Initial guess values of all variables (u, v, T,..., ε) in the cavity were given. (2) Eqs. (18)–(20) were computed for each wall in order to get the local radiative heat flux on the walls ($q_{rad\text{-}1}$, $q_{rad\text{-}3}$ and $q_{rad\text{-}4}$). (3) The conductive

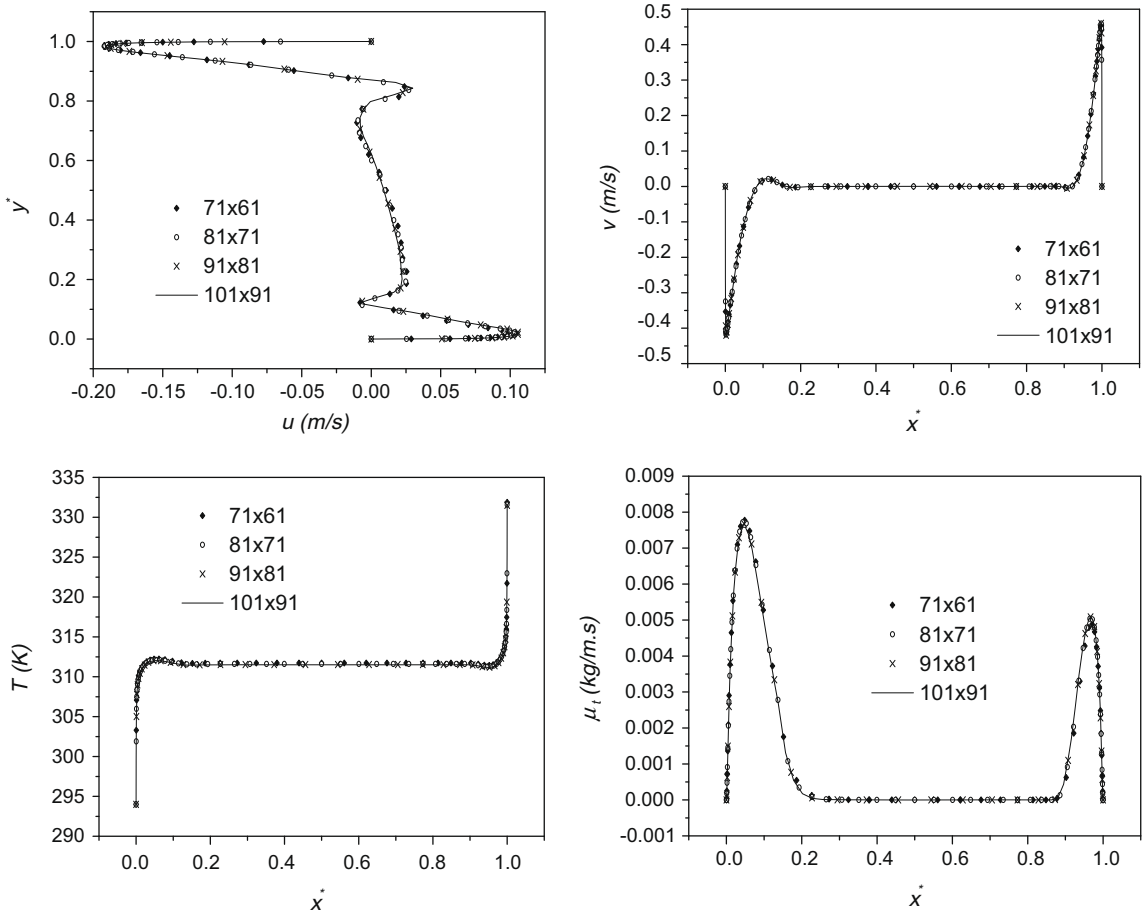

Fig. 3. Velocity components, temperature and turbulent viscosity for different grids at the center of the cavity.

model to obtain $q_{cond\text{-}g\text{-}4}$ was solved. (4) The pressure–velocity (u, v, p) were calculated by the SIMPLEC algorithm. (5) With the new calculated values of local radiative heat flux and velocity, the temperature (T), the turbulent kinetic energy (κ) and the turbulent dissipation of kinetic energy (ε) field in the cavity were obtained. (6) A convergence criterion was applied and (7) the process was repeated iteratively until the convergence criterion was achieved.

The accuracy of the numerical results was verified through numerous tests based on the grid size effect. The grid independence study was carried out for the largest cavity (6.98 m). The function used to generate the computational nodes in both directions "x" and "y" is presented below, where z_x is the stretching factor. On every computational run z_x had a value of 3.0, so for $L = 6.98$ m the first computation node was obtained at $x_i = 0.0014190$ m, and for $L = 0.70$ m the first node was to be at $x_i = 0.0001419$ m.

$$x_i = \frac{L}{2}\left\{1 + \frac{\tanh[2z_x(i/i_{\max} - 1/2)]}{\tanh(z_x)}\right\}$$

Fig. 3 shows the velocity components (u, v), temperature (T) and turbulent viscosity (μ_t) at the center of the cavity for different numerical grids. As we can see, there are minimum differences.

Table 1 presents the effect that the numerical meshes have on the average convective and radiative Nusselt number for $Ra = 10^{12}$. It can be seen that for a 91×81 mesh differences are lower than 1%. Therefore, a 91×81 grid was used for all cases considered herein. The discretization for the glass wall (6 mm) was always 10 nodes in the horizontal direction for all the meshes.

4.2. Validation of the numerical code

In order to validate the developed numerical code, two different turbulent convection problems are considered: (a) turbulent natural convection in a differentially heated square cavity and (b) turbulent natural convection with surface thermal radiation in a differentially heated square cavity. The comparison results are presented next.

4.2.1. Turbulent natural convection

The validation of the program was performed by comparing the numerical predictions with the experimental results for turbulent natural convection in a rectangular cavity by Ampofo and Karayiannis, 2003. The dimensions of the cavity were 0.75 m high, 0.75 m wide and 1.5 m deep. The hot and cold vertical walls of the cavity were isothermal at 50 and 10 °C respectively giving a Rayleigh number of 1.58×10^9. Other walls were insulated. The local velocity and temperature were simultaneously measured at different locations in the cavity using a laser Doppler anemometer (LDA) and a micro-diameter thermocouple.

Fig. 4 shows a comparison between the predicted and measured dimensionless vertical velocity and temperature profiles at the cavity mid-height. As observed in the figure, the predicted velocity profile agrees closely with the measured results. The predicted air temperature is also in excellent agreement with the measurement. It is observed that the experimental result (temperature) is not symmetrical at $y^* = 0.5$.

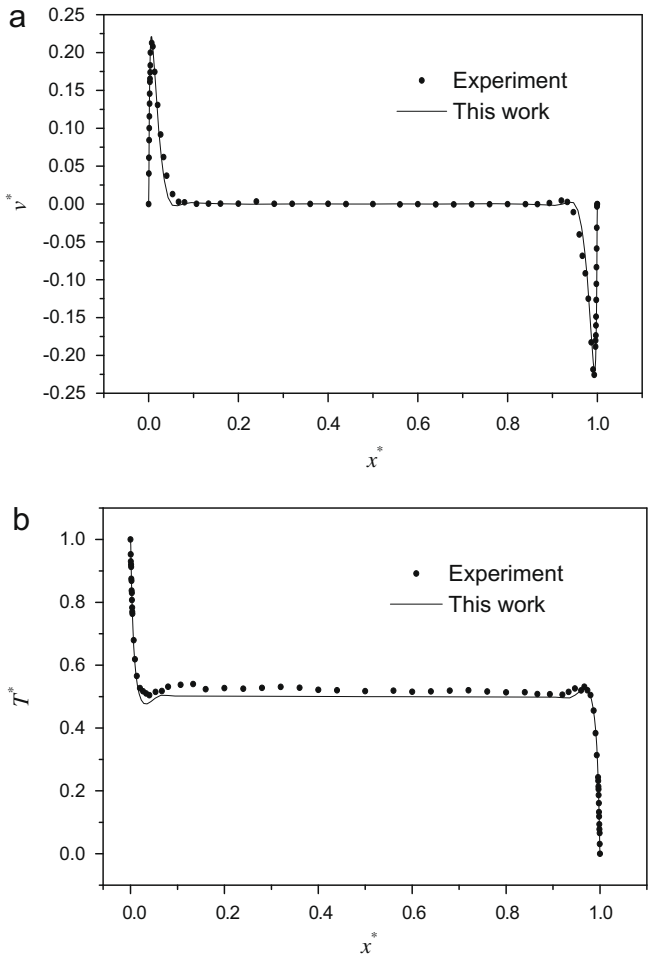

Fig. 4. Comparison of predicted and measured dimensionless (a) vertical velocity and (b) air temperature at the cavity mid-height.

Table 2 compares the present prediction of local Nusselt numbers with the experimental results reported by Ampofo and Karayiannis (2003). The local Nusselt numbers were calculated for the hot wall of the cavity. It is observed that the present predictions had a maximum absolute difference of 26.31%, this is near to the hot wall. This may occur due the lack of capacity to model tur-

Table 1
Average convective and radiative Nusselt numbers and its percentage difference for different numerical grids.

Grid	Nu_{conv}	% difference	Nu_{rad}	% difference
61×51	775.26		521.99	
71×61	817.34	5.15*	519.33	0.51*
81×71	832.18	1.78*	518.65	0.13*
91×81	833.20	0.12*	518.93	0.05*
101×91	833.92	0.09*	518.98	0.01*

Note. *Absolute difference in %.

Table 2
Comparison of present solution of local Nusselt numbers against those reported by Ampofo and Karayiannis (2003).

y^*	Ampofo et al. Experimental results	This work Numerical results	Absolute difference (%)
0.02	136.00	171.78	26.31
0.0493	122.00	136.60	11.96
0.1000	95.00	110.94	16.78
0.2000	84.00	86.22	2.64
0.3000	72.00	72.70	0.97
0.4000	65.00	70.53	8.51
0.5000	58.00	69.82	20.37
0.6000	52.00	64.11	23.29
0.7000	47.00	55.78	18.67
0.8000	40.00	45.04	12.61
0.9000	36.00	32.74	9.06
0.9493	28.00	25.28	9.72
0.9867	17.00	13.29	21.81
Nu_{ave}	65.54	73.45	12.07

bulent heat flux with the k-ε model, where the turbulent Prandtl number would not be constant close to the walls.

In the last line of the table, it is shown the comparison of the average Nusselt numbers; here the absolute difference is 12.07%, which can be considered the error of the turbulent model.

4.2.2. Turbulent natural convection and surface thermal radiation

The other selected problem to validate the numerical code was the conjugate heat transfer by turbulent natural convection and surface thermal radiation in a square cavity with differentially heated vertical walls, reported by Velusamy et al. (2001). The comparison was made with the following two cases: *case* 1 (the walls have an emissivity equal to 0.9, $T_H = 328$ K, $T_C = 318$ K and $Ra = 10^{11}$) and *case* 2 (the walls have an emissivity equal to 0.9, $T_H = 348$ K, $T_C = 298$ K and $Ra = 10^{11}$). Table 3 shows the results for both cases in terms of the average Nusselt numbers (convective (conv), radiative (rad) and total (total)) in the hot (h) and cold (c) walls. The maximum and minimum percentage differences observed for case 1 are 3.14% for $Nu_{c\text{-}conv}$ and 0.11% for $Nu_{h\text{-}rad}$, respectively. In case 2, the maximum percentage difference observed is 3.29% for $Nu_{c\text{-}conv}$ and the minimum percentage difference is 0.10% for $Nu_{h\text{-}rad}$. However, the percentage differences for the average total Nusselt numbers are 0.78% and 1.15% for case 1 and case 2, respectively. The observed differences for the average convective and radiative Nusselt numbers can be attributed to the stretching factor of the computational mesh used in the calculations. It is convenient to say that the convective Nusselt numbers are more sensitive to the grid size than to the radiative Nusselt numbers. On Fig. 5, turbulent viscosity with and without radiative exchange for case 1 is shown. From this figure it can be observed that, when radiation is taken into account, the turbulence level is higher compared to the case when only convection is considered. Turbulence effects also show up over the horizontal walls, where a very thick layer about 15% of the cavity height is formed; these effects make the velocity levels get higher, so does the boundary layer for the case when the radiative effect is taken into account.

From the above comparisons results, we considered our numerical code sufficiently tested.

5. Results and discussion

The parameters used to obtain the conjugate heat transfer results for the square cavity with a semitransparent wall using a solar control film are described next. The cavity lengths considered in this work are: 6.98 m ($Ra = 10^{12}$), 3.24 m ($Ra = 10^{11}$), 1.50 m ($Ra = 10^{10}$) and 0.70 m ($Ra = 10^{9}$). The Rayleigh number is based on the temperature difference between the vertical walls, using the mean temperature for the semitransparent wall with solar control coating. The solar radiation incoming in a normal direction over the semitransparent wall has a constant value of $G = 750$ W/m^2. The glass thickness was 6 mm with a selective coating film of SnS–Cu_xS whose properties were reported by Nair and Nair (1991) and are shown in Table 4. The isothermal wall temperature was taken as 21 °C (294 K). The external conditions around the semitransparent wall are: the external convection coefficient has a constant value of 6.8 W/m^2 K corresponding to an air velocity of 3 m/s and the ambient temperature has a fixed temperature of 35 °C (308 K) (warm climates). The emissivity of the semitransparent wall without the solar control film was 0.85 and when the solar control film is considered the emissivity diminishes to 0.4. The remaining walls have an emissivity equal to 0.9.

A description of the streamlines, isotherms and turbulent viscosity distributions for cases A (SCC) and B (WSCC) is presented only for a cavity with length equal to 6.98 m (corresponding to the upper limit of *Ra* considered in this study) but the heat transfer parameters are presented for every length considered in this work.

Table 3
Comparison of the present study with reported results by Velusamy et al. (2001) for the natural convection and radiation in a square cavity.

	Case 1		Case 2	
	Velusamy et al.	This work[a]	Velusamy et al.	This work[a]
$Nu_{h\text{-}conv}$	334.90	345.22 (3.08%)	326.03	336.30 (3.15%)
$Nu_{c\text{-}conv}$	339.34	349.98 (3.14%)	344.57	355.89 (3.29%)
$Nu_{h\text{-}rad}$	873.58	872.66 (0.11%)	523.06	522.52 (0.10%)
$Nu_{c\text{-}rad}$	869.14	867.52 (0.19%)	504.52	502.89 (0.32%)
Nu_{total}	1208.5	1217.88 (0.78%)	849.09	858.82 (1.15%)

[a] The values among parenthesis are percentage absolute differences.

Table 4
Optical and thermophysical properties of glass and SnS–Cu_xS solar control coating.

Glass (6 mm)	Film (SnS–Cu_xS)	(Glass–film)
$\alpha_g^* = 0.14$	$A^* = 0.64$	$\alpha_{ysst}^* = \alpha_g^* + \alpha_f^* = 0.69$
$\tau_g^* = 0.78$	$T^* = 0.20$	$\tau_{syst}^* = 1 - \alpha_{sist}^* - \rho_{sist}^* = 0.15$
$\rho_g^* = 0.08$	$R^* = 0.16$	$\rho_{syst}^* = R^*/100 = 0.16$
$\varepsilon_g^* = 0.85$	$\varepsilon_f^* = 0.40$	
$\lambda_g = 1.4$ W/m K	$\alpha_f^* = (1 - \alpha_g^*)A^*/100 = 0.55$	
$Cp_g = 750$ J/kg K	$\tau_f^* = \tau_{sist}^*/\tau_g^* = 0.19$	
$\rho_g = 2500$ kg/m^3	$\rho_f^* = 1 - \tau_f^* - \alpha_f^* = 0.26$	

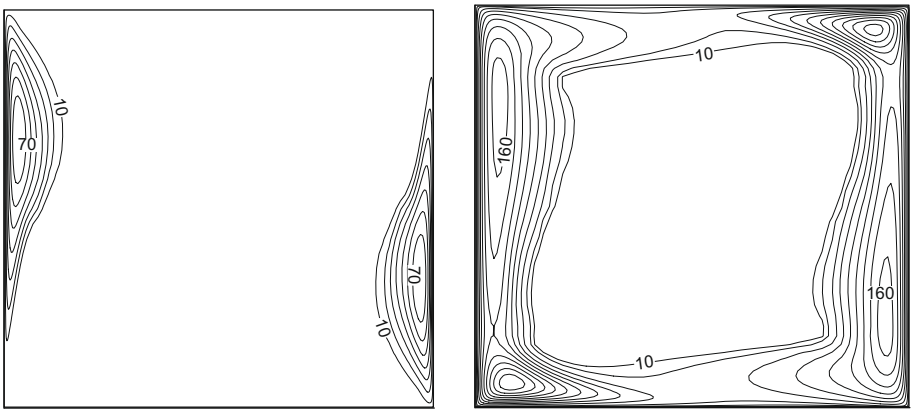

(a) without radiation (b) with radiation

Fig. 5. Dimensionless turbulent viscosity (μ_t/μ): (a) turbulent natural convection and (b) turbulent natural convection-surface thermal radiation.

5.1. Streamlines, isotherms and turbulent viscosity patterns results

In Fig. 6, the streamlines (top), isotherms (middle) and turbulent viscosity (bottom) distributions are presented for case A, glazing with *s*olar *c*ontrol *c*oating (SCC) and case B, glazing *w*ithout *s*olar *c*ontrol *c*oating (WSCC). The streamlines show, in both cases A and B, a counterclockwise air movement from semitransparent wall (right) to isothermal wall (left). The flow pattern is caused by the heat transferred to the adjacent air of the semitransparent wall, increasing its temperature and forming an ascending motion impelled by the buoyancy force. In both cases, at the center of the cavity, the streamlines are horizontal, indicating fluid stratification, but at the boundaries adjacent to the adiabatic walls there are significant differences. At the top of the adiabatic wall the spaces between the streamlines are different for cases A and B. For case A the streamlines are closer between them, thus indicating

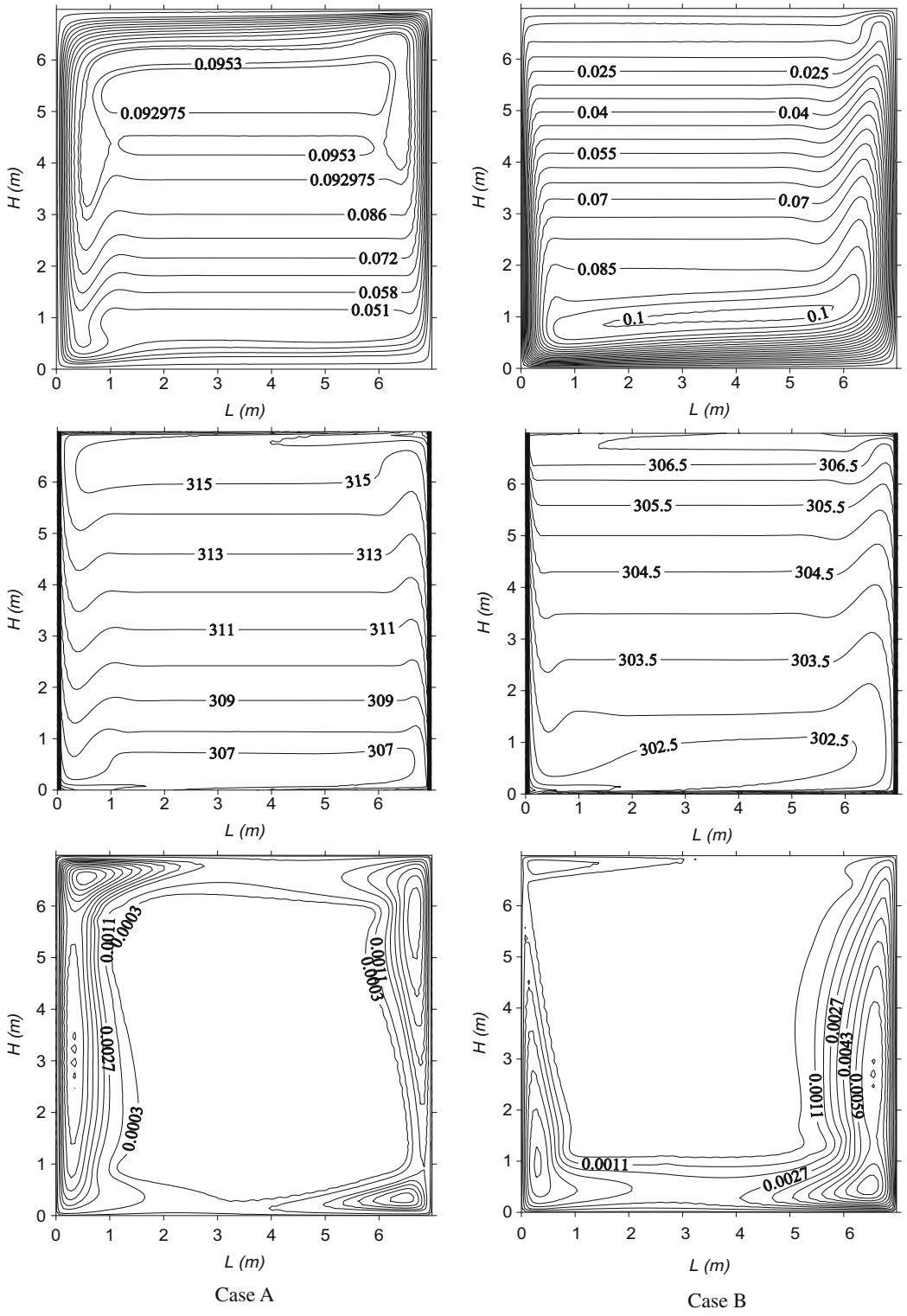

Fig. 6. Streamlines (m^2/s), isotherms (K), and turbulent viscosity (m^2/s) for case A and case B.

higher buoyancy forces, contrary to case B, and at the bottom of the adiabatic wall it is the opposite; the spaces between the streamlines at the bottom are closer for case B, contrary to case A. Also, for case A, the streamline vortex is at top of the cavity contrary to case B, which is at the bottom of the cavity. Thus, we can see that the effect of solar control coating attached to glass changes the movement of air inside the cavity.

The isotherm distributions for cases A and B (cavities shown at the middle of Fig. 6) present stratification about 60% of the cavity. As we can see, the temperature values are higher for case A than for case B. Comparing the difference of temperature values of the isotherms for cases A and B close to the bottom and at the top, we can find that the difference increases as the height of the cavity increases, from 4.5 °C at the bottom to 8.5 °C at the top. The explanation of the increase of temperatures in case A compared to case B shall be given further on.

The turbulence viscosity distribution (cavities shown at the bottom of Fig. 6) indicates that the higher turbulent levels are close to the boundaries of the vertical walls for both cases. For case A, higher turbulence levels show at the upper wall of the cavity ($y > 6.0$ m) and lower values are at the lower wall. On the contrary, for case B higher turbulence levels can be seen at the lower wall of the cavity ($y < 0.95$ m) compared to the ones at the upper wall, where turbulence viscosity is almost negligible; this explains the vortex flow at the top of the cavity in case A and at the bottom in case B.

In Fig. 7, the temperature distribution of the inside and outside surfaces of the semitransparent wall is shown for both cases. For case A, the temperature values at the inside surface are higher, since the solar control film coating is adhered on glass, it absorbs 55% of solar energy ($\alpha_f^* = 0.55$) against the clear glass ($\alpha_g^* = 0.14$), which absorbs 14%. For case B, the outside surface temperatures of the glass are slightly higher than those of the inside surface of the glass. The temperature difference between the top and the bottom of the vertical semitransparent wall for case A was nearly 6 °C and for case B was 2 °C. The average temperature difference between the inside and outside surfaces of the semitransparent wall for case A was around 1.07 °C and for case B was 0.04 °C. For case A, the inside average temperature on the semitransparent wall was 59 °C and for case B was 38.5 °C. It was reported from Xamán and Álvarez (2006) that for the same conditions, but without the radiative exchange between surfaces in the cavity, the inside average temperature for the semitransparent wall with solar control film coating was 64 °C and for the plain semitransparent wall was 40 °C. Thus, if we include the radiative exchange between walls the temperatures of the film coating and the plain glass change. Also, it can be seen that the strong variation of the temperature (~3 °C) at the upper side of the semitransparent wall for case A ($y^* > 0.9$) contributes to the vortex that appears at the top of the cavity (see streamlines in Fig. 6). Similarly for case B, the interior temperature variation (~1 °C) at the lower side of the semitransparent wall ($y^* < 0.1$) contributes to the vortex that makes the inside fluid at the lower region of the cavity to form recirculation.

In Fig. 8, the local convective, radiative and total heat transfer fluxes going to the inside of the cavity from the semitransparent wall with SCC (case A) and WSCC (case B) walls are presented.

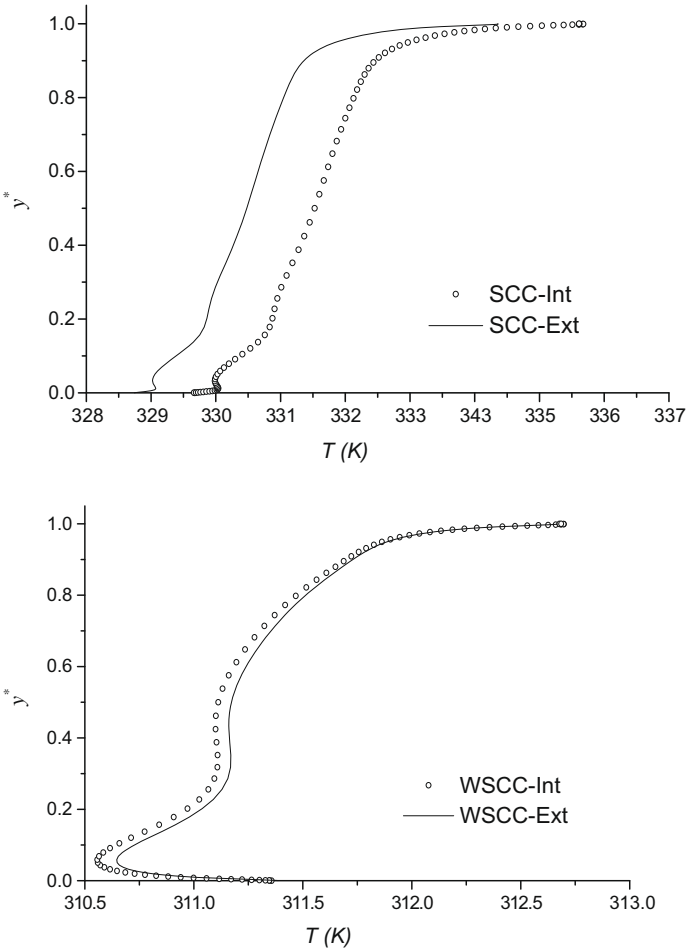

Fig. 7. Interior and exterior temperatures of the semitransparent wall with solar control coating (SCC) and without solar control coating (WSCC).

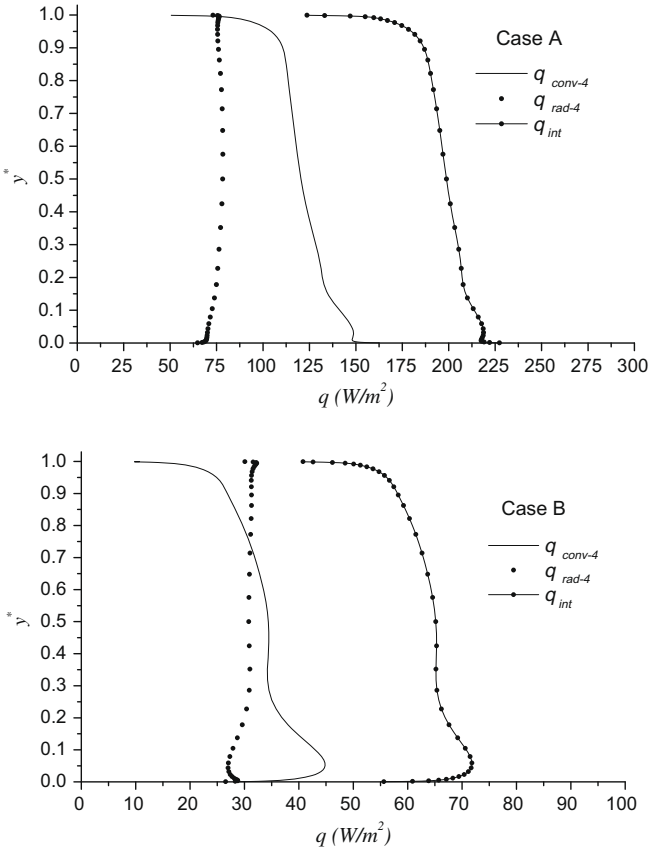

Fig. 8. Local convective, radiative and total heat fluxes distribution from the SCC and WSCC walls to the interior cavity.

For case A, the convective heat transfer fluxes are higher than the radiative heat transfer fluxes, but for case B, the difference between the convective and radiative heat fluxes diminishes. Particularly for case B, the convective heat transfer flux is higher until $y^* \sim 0.75$ compared to the radiative heat flux. The solar control film coating temperatures of the semitransparent wall causes an increase of the convective and radiative heat fluxes. The average heat flux going inside the cavity by natural convection and surface thermal radiation is 217.65% higher for case A than that of case B.

In Table 5, the average heat transfer fluxes and the solar heat gain coefficient (SHGC) of semitransparent wall for cases A and B are presented. The used nomenclature is as follow: q_τ = transmitted heat flux through the semitransparent wall toward the interior of the cavity, q_α = absorbed heat flux by the semitransparent wall, q_ρ = reflected heat flux to cavity outside, q_{int} = inside heat flux by natural convection and thermal radiation from the semitransparent wall to the cavity, q_{out} = outside heat flux by natural convection and thermal radiation from the semitransparent wall toward the outside of the cavity, $q_{int} + q_\tau$ = inside total heat flux, $q_{out} + q_\rho$ = outside total heat flux and q_{total} = net heat flux. A total energy balance was carried out, where a difference of 0.026% was obtained for case A and 0.036% for case B, showing in consequence that the energy balance was archived. As we can see, the SHGC calculated by Eq. (24) for case B is higher (86.17%) than case A (44.19%). This indicates that from the 100% of the solar energy that strikes the glazing, only 44.19% of the total heat flux goes through the glass with SnS–Cu_xS solar control film coating, while 86.17% goes through the plain glass. Thus, for the glazing with SnS–Cu_xS solar control coating, the energy gains toward the interior decreases by 41.98%. These results will allow us to look to the advantage of solar control film coatings on glazing.

From Table 5, we also can see that the total heat flux inside the cavity for case A (331.44 W/m^2), is lower than for case B (646.24 W/m^2). Nevertheless, for case A, even though the total heat flux is lower; higher air temperature inside the cavity is reached. The result above-mentioned is explained as follow: from the total heat flux of 331.44 W/m^2 going into the cavity, only 137.29 W/m^2 (q_τ) hits directly on the isothermal wall (cold wall), since the absorptance is $\alpha^* = 0.90$, this wall absorbs 90% (123.56 W/m^2) of the direct radiative energy; so the effective energy going into the cavity for case A is: $q_{\text{int}} + (q_\tau - \alpha^* q_\tau) = 194.15 + 13.73 = 207.88$ W/m^2. Likewise, the effective energy inside the cavity for case B is: $q_{\text{int}} + (q_\tau - \alpha^* q_\tau) = 61.12 + 58.61 = 119.73$ W/m^2. For this reason, because the 0.9 absorptance of the isothermal wall, the energy contribution going inside the cavity with a solar control film coating semitransparent wall is apparently higher.

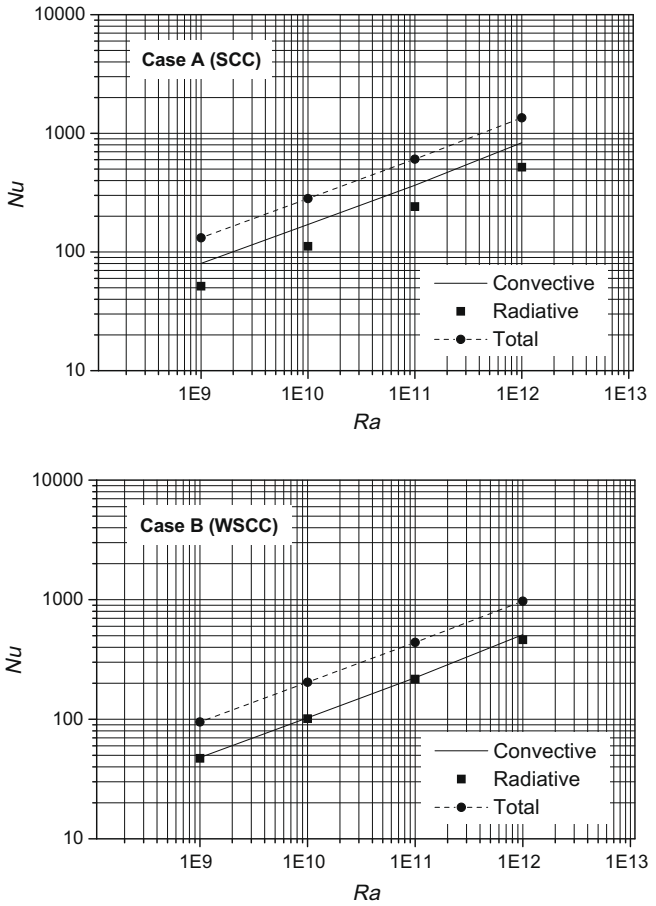

Fig. 9. Average convective, radiative and total Nusselt number for the case A and B for $10^9 \leqslant Ra \leqslant 10^{12}$.

Table 5
Average heat fluxes (W/m^2) for cases A and B.

Case	q_τ	q_α	q_ρ	q_{int}	q_{out}	$q_{int} + q_\tau$	$q_{out} + q_\rho$	q_{total}	G	SHGC (%)
A	137.29	492.49	120	194.15	298.36	331.44	418.36	749.80	750	44.19
B	585.12	104.61	60	61.12	43.49	646.24	103.49	749.73	750	86.17

Table 6
Comparison between the present study (cases A and B) and the reported results by Velusamy et al. (2001).

Ra	Nu_{conv}			Nu_{rad}			Nu_{total}		
	[Ref.]	Case A	Case B	[Ref.]	Case A	Case B	[Ref.]	Case A	Case B
10^{09}	69.04	80.21 (16.19%)	47.87 (30.66%)	112.39	51.54 (54.14%)	47.07 (58.12%)	181.43	131.75 (27.38%)	94.94 (47.67%)
10^{10}	151.28	170.29 (12.57%)	102.94 (31.95%)	242.68	111.69 (53.98%)	101.00 (58.38%)	393.96	281.98 (28.42%)	203.94 (48.23%)
10^{11}	326.03	364.71 (11.86%)	222.71 (31.69%)	523.06	241.80 (53.77%)	216.68 (58.57%)	849.09	606.51 (28.57%)	439.39 (48.25%)
10^{12}	726.07	833.19 (14.75%)	510.61 (29.67%)	1128.20	518.93 (54.00%)	461.90 (59.06%)	1854.30	1352.12 (27.08%)	972.51 (47.55%)

Note. The values in () are the absolute difference in %.

5.2. Nusselt number results

Fig. 9 shows the average convective, radiative and total Nusselt numbers as a function of Rayleigh Number for cases A and B. For case A, the average radiative contribution to total Nusselt number is about 39%, while for case B it's about 50%, hence demonstrating the importance of considering the surface thermal radiation in this problem.

Using least square regression, a set of correlations for the average Nusselt number for cases A and B for $10^9 < Ra < 10^{12}$ are introduced:

Case A

$$Nu_{conv} = 0.0716Ra^{0.338} \quad (28)$$

$$Nu_{rad} = 0.0505Ra^{0.3344} \quad (29)$$

$$Nu_{total} = 0.1219Ra^{0.3366} \quad (30)$$

Case B

$$Nu_{conv} = 0.0395Ra^{0.3419} \quad (31)$$

$$Nu_{rad} = 0.0498Ra^{0.3307} \quad (32)$$

$$Nu_{total} = 0.0884Ra^{0.3365} \quad (33)$$

The above Nusselt number correlations show a maximum percentage difference of 1.3% (case A) and 1.2% (case B) against the numerical results.

Additionally, the convective and radiative Nusselt number results for both cases, A and B were compared to the ones presented by Velusamy et al. (2001) (Table 6). This author's results are for a differentially heated squared cavity problem, in which natural convection and radiative exchange between surfaces was considered for a temperature difference between vertical walls of 50 K and walls emissivity of 0.9. From this table, it can be observed that convective Nusselt number for the cavity with a semitransparent wall with SCC (case A) is higher compared to the convective Nusselt number of Velusamy et al., where the maximum difference is 16.19%, whereas for case B, the convective Nusselt number is lower, with a maximum difference of 31.95%. The radiative Nusselt numbers for both cases A and B are lower than the ones reported by Velusamy et al. (2001).

Summarizing, for cases A and B, the maximum difference of the total Nusselt number reported from Velusamy et al. was 28.57% and 48.25%, respectively. The reason for these differences is the temperature distribution of the semitransparent wall for cases A and B.

6. Conclusions

This paper presents a numerical study of the conjugate heat transfer (natural convection, surface thermal radiation and conduction) in a square cavity with turbulent flow. The cavity has one vertical isothermal wall, two horizontal adiabatic walls and one vertical semitransparent wall with a SnS–Cu_xS solar control film coating applied to control the solar radiation transmission. The numerical code was verified and validated by reducing it to cases previously reported in the literature, obtaining a good agreement.

By using the solar control film coating on the semitransparent wall, the total heat flux was reduced from 646.24 (case B) to 331.44 W/m^2 (case A), even though the temperatures of the film coating on the semitransparent wall (case A) were higher than the ones obtained without solar control film (case B). On the other hand, for case A, the solar heat gain coefficient (SHGC) was 44.19% and for case B was 86.17%, a decrease of 41.98% was obtained.

Also Nusselt number correlations as a function of Rayleigh number are presented for the studied cavities (case A and case B). These correlations can be applied to determine the combined convective and radiative Nusselt number coefficients separately and the heat fluxes in cavities. Furthermore, these correlations may be used to provide information to commercial software as DOE-2 or TRNSYS, in order to determine the average thermal loads in rooms.

Finally, the developed two-dimensional numerical model of conjugate turbulent heat transfer in a cavity with semitransparent wall was capable of studying in detail the fluid flow and heat transfer phenomena. This may represent an advance in the knowledge of what we can have in real rooms with a window having or not, solar control film coating.

In the near future, a parametric study will be needed in order to provide more information about other type of film coatings.

Acknowledgment

The authors wish to thank the constant emotional support provided by IBM and Studentship support from CONACYT and SEP from México.

References

Álvarez, G., Estrada, C., 2000. Numerical heat transfer in a cavity with a solar control coating deposited to a vertical semitransparent wall. Int. J. Numer. Meth. Fluids 34, 585–607.

Ampofo, F., Karayiannis, T., 2003. Experimental benchmark data for turbulent natural convection in an air filled square cavity. Int. J. Heat Mass Transfer 46, 3551–3572.

Anil Kumar Sharma, Velusamy, K., Balaji, C., Venkateshan, S.P., 2007. Conjugate turbulent natural convection with surface radiation in air filled rectangular enclosures. Int. J. Heat Mass Transfer 50, 625–639.

ASHRAE Handbook Fundamentals, 2005. American Society if Heating Refrigeration and Air-Conditioning Engineers Inc.

Behnia, M., Rizes, J., De Vahl Davis, G., 1990. Combined radiation and natural convection in a cavity with a transparent wall and containing a non-participant fluid. Int. J. Numer. Meth. Fluids 10, 305–325.

Henkes, R., Van-Der-Vlugt, F., Hoogendoorn, C., 1991. Natural-convection flow in a square cavity calculated with low-Reynolds-number turbulence models. Int. J. Heat Mass Transfer 34, 377–388.

Kwon, S., Kwon, Y., Park, J., 1993. Numerical study of combined natural convection and radiation in a rectangular enclosure with a transparent window on the center region of right wall. In: Proceedings of the Sixth International Symposium on Transport Phenomena in Thermal Engineering, Seoul, Korea, pp. 299–304.

Larson, D., Viskanta, R., 1976. Transient combined laminar free convection and radiation in a rectangular enclosure. J. Fluid Mech. 78, 65–85.

Modest, M., 1993. Radiative Heat Transfer. McGraw-Hill, New York.

Mallison, G.D., de Vahl Davis, G., 1973. The method of false transients for the solution of coupled elliptic equations. J. Comput. Phys. 12, 435–461.
Nair, M., Nair, P., 1991. SnS–Cu_xS thin film combination: a desirable solar control coatings for architectural and automobile glazings. J. Phys. D: Appl. Phys. 24, 450–453.
Oosthuizen, P., Naylor, D., 1999. Introduction to Convective Heat Transfer Analysis. McGraw-Hill, New York.
Patankar, S., 1980. Numerical Heat Transfer and Fluid Flow. Hemisphere Publishing Corporation, Washington, DC.
Pope, S., 2000. Turbulent Flows. Cambridge University Press, UK.
Van Doormaal, J., Raithby, G., 1984. Enhancements of the SIMPLE method for predicting incompressible fluid flow. Numer. Heat Transfer 7, 147–163.
Velusamy, K., Sundararajan, T., Seetharamu, K., 2001. Interaction effects between surface radiation and turbulent natural convection in square and rectangular enclosures. J. Heat Transfer 123, 1062–1070.
Webb, B., Viskanta, R., 1987. Radiation-induced buoyancy-driven flow in rectangular enclosures: experiment and analysis. J. Heat Transfer 109, 427–433.
Xamán, J., Álvarez, G., 2006. Effect of heat conduction of SnS–Cu_xS solar control coated semitransparent wall on turbulent natural convection in a square cavity. Numer. Heat Transfer Part A 50, 79–98.
Xamán, J., Arce, J., Álvarez, G., Chávez, Y., 2008. Laminar and turbulent natural convection combined with surface thermal radiation in a square cavity with a glass wall. Int. J. Therm. Sci. 47, 1630–1638.